Superconductor Science and Technology

PAPER • **OPEN ACCESS**

Magnetic flux penetration into micron-sized superconductor/ferromagnet bilayers

OPEN ACCESS
IOP Publishing
Superconductor Science and Technology
Supercond. Sci. Technol. 33 (2020) 025015 (7pp)
https://doi.org/10.1088/1361-6668/ab54ab

Magnetic flux penetration into micron-sized superconductor/ferromagnet bilayers

J Simmendinger[1,3], M Weigand[1], G Schütz[1] and J Albrecht[2]

[1] Max Planck Institute for Intelligent Systems, Heisenbergstr. 1, D-70569 Stuttgart, Germany
[2] Research Institute for Innovative Surfaces FINO, Beethovenstr. 1, D-73430 Aalen, Germany

E-mail: simmendinger@is.mpg.de

Received 19 June 2019, revised 10 October 2019
Accepted for publication 5 November 2019
Published 14 January 2020

Abstract

Flux penetration into small superconductor/ferromagnet elements is investigated by magneto-optical imaging and magnetic scanning transmission x-ray microscopy at low temperatures. It is found that penetration of magnetic flux into a thin bilayer of YBCO and Py strongly depends on the direction of a perpendicular magnetic field. The soft-magnetic layer acts as an amplifier for magnetic in-plane components that are generated by electric currents in the superconductor. These in-plane components point in opposite direction above the ferromagnet and below the superconductor. As a consequence a strong inclination of the local magnetic field occurs that significantly slows down or speeds up the flux penetration into such elements. From detailed magnetic scanning x-ray microscopy results it is found that the effect dramatically increases if the elements get smaller. In $20 \times 20\,\mu m^2$ superconducting squares we observe magnetic flux penetration that differs by more than a factor of four when reversing the external magnetic field.

Keywords: flux penetration, superconducting thin films, magnetic x-ray microscopy, superconductor/ferromagnet structures

(Some figures may appear in colour only in the online journal)

Superconducting materials in external magnetic fields exhibit a diamagnetic response. This is originated by electric supercurrents that are induced and magnetically screen the volume of the superconductor. In type-II-superconductors this screening is provided by critical currents flowing in vortex penetrated parts of the material when the lower critical field is exceeded. The magnitude of the critical current and, thus, the required volume for current flow is determined by pinning of vortices [1, 2]. Experimentally, magnetic flux penetration into type-II-superconductors and the correlated flux pinning is often investigated by dichroic microscopy both in the optical frequency range [3] and in the soft x-ray regime using transmission microscopy [4], total electron yield [5–7] or photo electron emission microscopy [8]. In case of thin superconducting films the quantitative analysis of such measurements with the goal to extract the local critical current density can be performed with high accuracy [3], in particular, when considering the coupling of the stray field of the superconductor and the used ferromagnetic detector [9].

In this work we consider flux penetration into thin bilayers of superconductors and soft ferromagnets. In the present study we investigate thin film elements consisting of optimally doped high-temperature superconducting $YBa_2Cu_3O_{7-\delta}$ (YBCO) and permalloy ($Ni_{0.8}Fe_{0.2}$, Py). Systematic measurements have been performed on structures of constant thickness and different lateral sizes. Macroscopic elements are investigated by magneto-optical imaging, small squares with a dimension of $20 \times 20\,\mu m$ [2] are analyzed by means of magnetic scanning transmission x-ray microscopy (MSTXM). Advantages and disadvantages in comparison to established methods are discussed in [4].

It is observed that flux penetration into these structures differs from regular behavior. Flux penetration is not symmetric with respect to the orientation of the externally applied perpendicular field. The effect is rather small for elements in the

[3] Author to whom any correspondence should be addressed.

millimeter range and gets tremendously large when the aspect ratio between lateral size and thickness of the element is reduced. Thinking about the numerous applications of micron-sized superconducting thin films, e.g. SQUIDS [10] or microwave resonators [11, 12], the introduction of an additional soft-magnetic layer substantially modifies the flux distribution in the superconductor [13] leading to a different response depending on the direction of the external magnetic field. Furthermore, this effect has relevant consequences for a quantitative description of the evolving critical state in an external magnetic field.

Bilayers consisting of a ~430 nm thick YBCO film and a 50 nm thick soft-ferromagnetic Py layer are prepared in a two-step process. Optimally doped YBCO films are grown on a 5×5 mm^2 single-crystalline (100)-oriented $SrTiO_3$ (STO) substrate by pulsed laser deposition from a mixed target of 95 mol% YBCO and 5 mol% BYNTO, as described by Opherden *et al* [14] and Sieger *et al* [15]. Subsequent annealing in oxygen leads to strong pinning YBCO:BYNTO thin films with a typical transition temperature of $T_c = 90$ K and an extremely high critical current density [14–17]. This provides excellent conditions for successful dichroic imaging. In order to exploit the x-ray magnetic circular dichroism (XMCD) effect for nanoscopic x-ray imaging a ferromagnetic layer is sputtered directly on top of the superconductor. We use Py due to its small and temperature independent coercive field [4, 18, 19] to detect the local magnetic stray field of the supercurrents. A protection layer consisting of 10 nm MgO is placed in between superconductor and sensor layer to reduce the impact of pair-breaking effects [20].

For large thin film elements with lateral sizes of 100 μm and above the analysis is performed using the magneto-optical imaging technique. In particular, we use ferromagnetic iron garnet films as field-sensing layers that allow the mapping of the local magnetic field density distribution with a spatial resolution of about 5 μm [21]. A detailed description on the method is found in the review article of Jooss [3]. However, in this work we focus only on the determination of the flux density distribution at the surface of the superconductor.

When the lateral sizes of the bilayer elements get smaller than 100 μm the magneto-optical method does not provide satisfactory data. This gap can excellently be filled using MSTXM [4]. The x-ray method with its structural and magnetic spatial resolution of below 30 nm [22] and 100 nm [4], respectively, is most qualified to investigate the temperature and magnetic field dependence of flux penetration at low temperatures [23]. The MSTXM measurements are performed in the x-ray microscope MAXYMUS located at Bessy II in Berlin. The setup includes a liquid helium cryostat with a base-temperature of $T = 20$ K and a magnet system to apply fields up to $\mu_0 H = 40$ mT. For transmission measurements the access to a thin perovskite layer is necessary due to large absorption coefficients in the soft x-rays regime. Since YBCO:BYNTO thin film can only be grown on single-crystalline substrates, the substrate thickness is reduced after the growth process by focused ion-beam milling [24] to below 600 nm. A sketch of the sample is depicted in figure 1.

The so prepared samples are investigated by MSTXM at low temperatures as follows: first, the Py layer is characterized

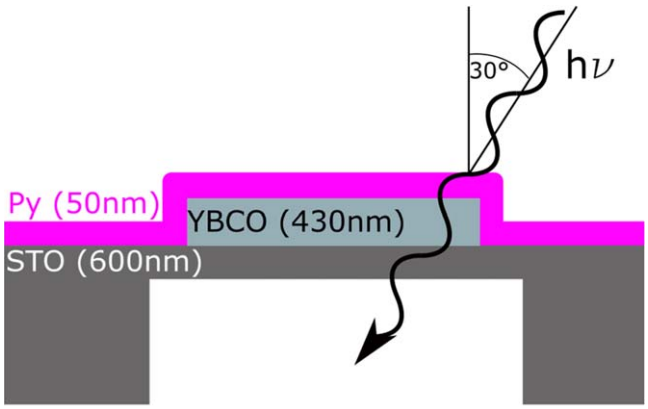

Figure 1. Cross-section sketch of the YBCO/Py heterostructure. The YBCO film is patterned to 20×20 μm^2 squares, subsequent a 50 nm Py sensor layer is sputtered directly on top before the substrate is locally thinned by focus ion-beam irradiation to enable transmission of x-ray radiation. To obtain the in-plane component of the measuring signal an incident angle of 30° is used.

at $T = 100$ K to access magnetic properties slightly above the superconducting transition. Therefore, we measured the magnetic response of the ferromagnetic layer with MSTXM for varying in-plane fields $B_{\mathrm{ext},x}$ which were applied in in x-direction. The averaged signal for a single SC/FM square as function of $B_{\mathrm{ext},x}$ is displayed in figure 2, together with exemplary images at $B_{\mathrm{ext},x} = -1$ mT; -0.5 mT; 0 mT; 0.5 mT; 1 mT.

There is a smooth change in the magnetization from the initial magnetization (blue) towards the reversed magnetization (red) with a coercive field of less than 0.5 mT. This value is in good agreement with both SQUID magnetometry measurements [4] and literature values [18, 19]. As visualized by the non-uniform color distribution in the image taken at 0 mT, the sample exhibits a multi-domain state in zero field. There are blue artifacts in the images for positive fields that correspond to surface structures of the superconductor [23]. The structures are seen in detail in the scanning electron micrograph on the bottom right. Since these artifacts only occur in vicinity of $B = 0$ mT, these effects were omitted in this work; however, detailed knowledge of these effects is highly desired.

In the following we assume that the ferromagnet solely interacts with the superconductor via magnetic dipolar coupling [25–27]. The complex interaction in SC/FM compounds is discussed in more details by Stahl *et al* [28, 29].

The properties of the YBCO/Py bilayer are now addressed at a temperature of $T = 26$ K after zero-field cooling. The superconducting element is prepared into the critical state by applying an out-of-plane field of $B_{\mathrm{ext},\perp} = 40$ mT. As imaged by MSTXM in figure 3, supercurrents flow throughout the whole film leading to a roof-top geometry with d-lines [30] along the diagonals.

The superconducting sample appears in a multicolored state. There are triangular shaped areas on the left and on the right that exhibit blue and red color, respectively. Top and bottom areas appear yellow. This can be understood when regarding the supercurrent flow and the related magnetic field distribution in a square-shaped film. The current stream lines are concentric squares. Therefore, the corresponding in-plane

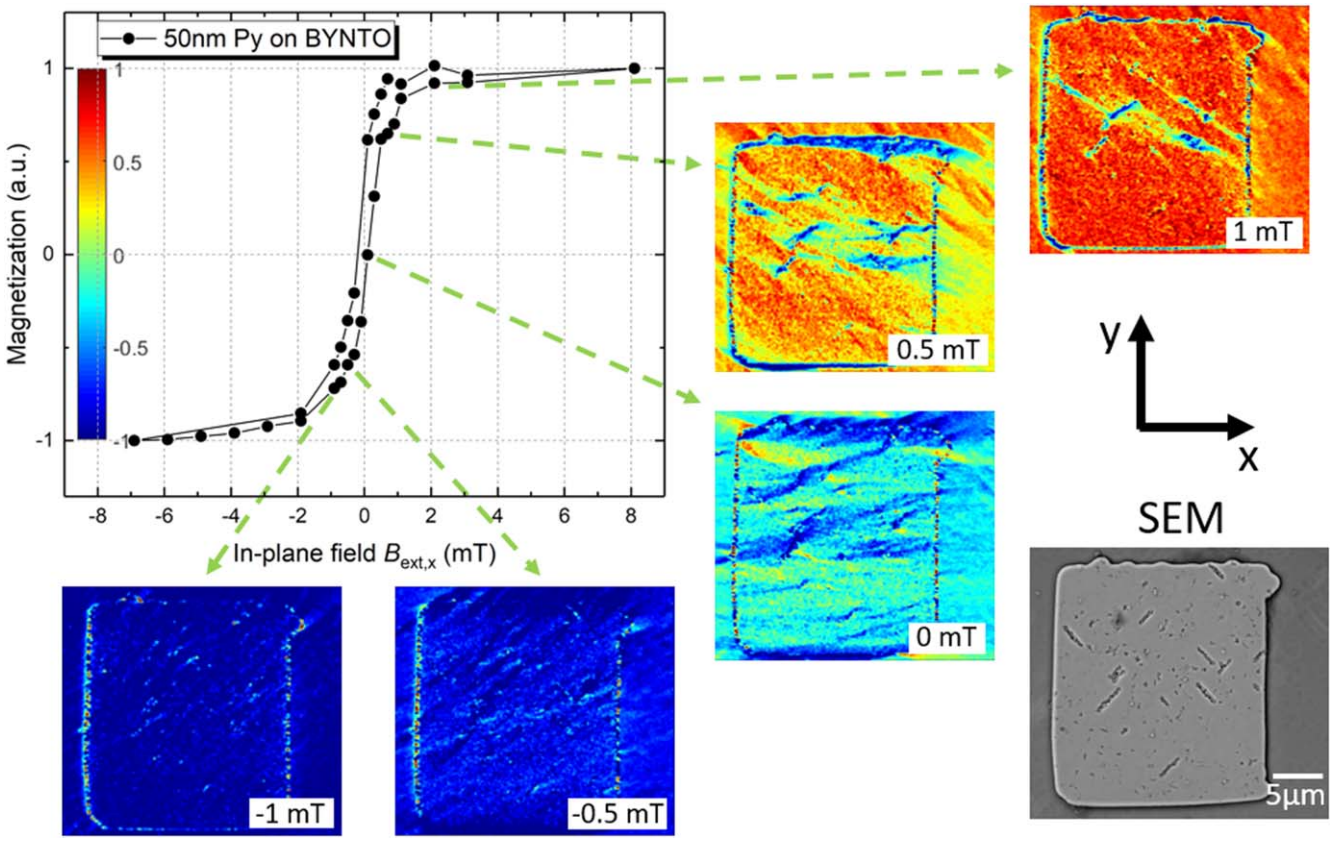

Figure 2. Local in-plane hysteresis of the soft magnetic Py layer at $T = 100$ K. The magnetization signal is averaged over the 20×20 μm square. With the YBCO in the normal conducting state solely the magnetic properties of the Py film are probed. We find a coercive field below 0.5 mT. In addition, nearly no pinning of domain walls at surface structures of the YBCO film is observed. (Bottom right) SEM picture of the YBCO surface.

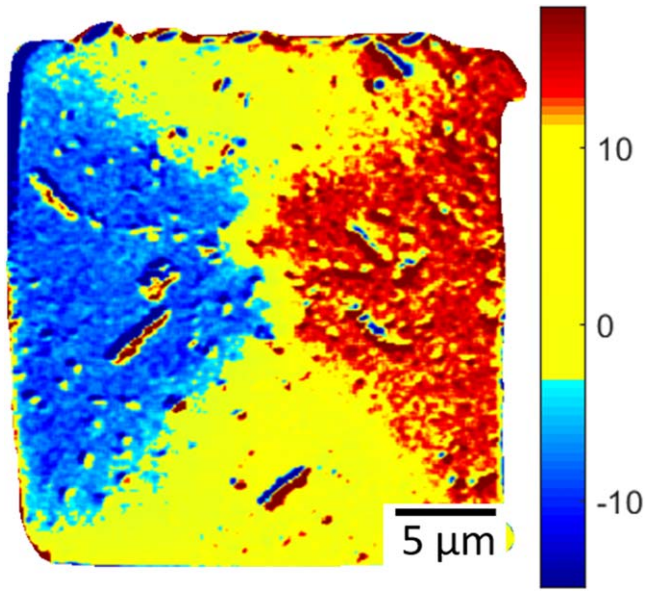

Figure 3. MSTXM image of a 20×20 μm^2 YBCO thin film in the critical state ($B_{ext,\perp} = 40$ mT) at $T = 26$ K. The color scale refers to the XMCD signal in %. The magnetic data exhibit the expected four-fold symmetry indicating homogeneous current distribution throughout the whole square.

field components (measured signal) point to the edges of the film forming four triangular-shaped domains [3, 30–32].

The MSTXM method is only sensitive to magnetic fields with a finite component along the incident vector of the x-ray beam. The used color code shows the *x*-component (oriented horizontally in the image) of the magnetic signal, which solely has finite values in the left and right triangular domains. The image in figure 3 reveals that the superconducting properties of the investigated element are homogeneous because the x-ray image shows the expected four-fold symmetry.

In a next step, the response of the SC/FM element to an externally applied field $B_{ext,\perp}$ is investigated to analyze the evolution of magnetic flux fronts. For that purpose, the ferromagnetic layer is set into the remanent state at $T = 95$ K (normalized XMCD = 1, red color) before cooling the element down to $T = 39$ K in zero-field. Subsequently, a finite $B_{ext,\perp}$ is applied to force magnetic flux to penetrate from the edges into the sample.

As it is depicted in the top row of figure 4, flux starts to penetrate from the edges of the square (blue area) into the virgin (flux free) superconductor, reaching complete penetration at $B_{ext,\perp} = 40$ mT. Here, the type-II- superconductor is completely in the mixed-state with supercurrents circulating clockwise.

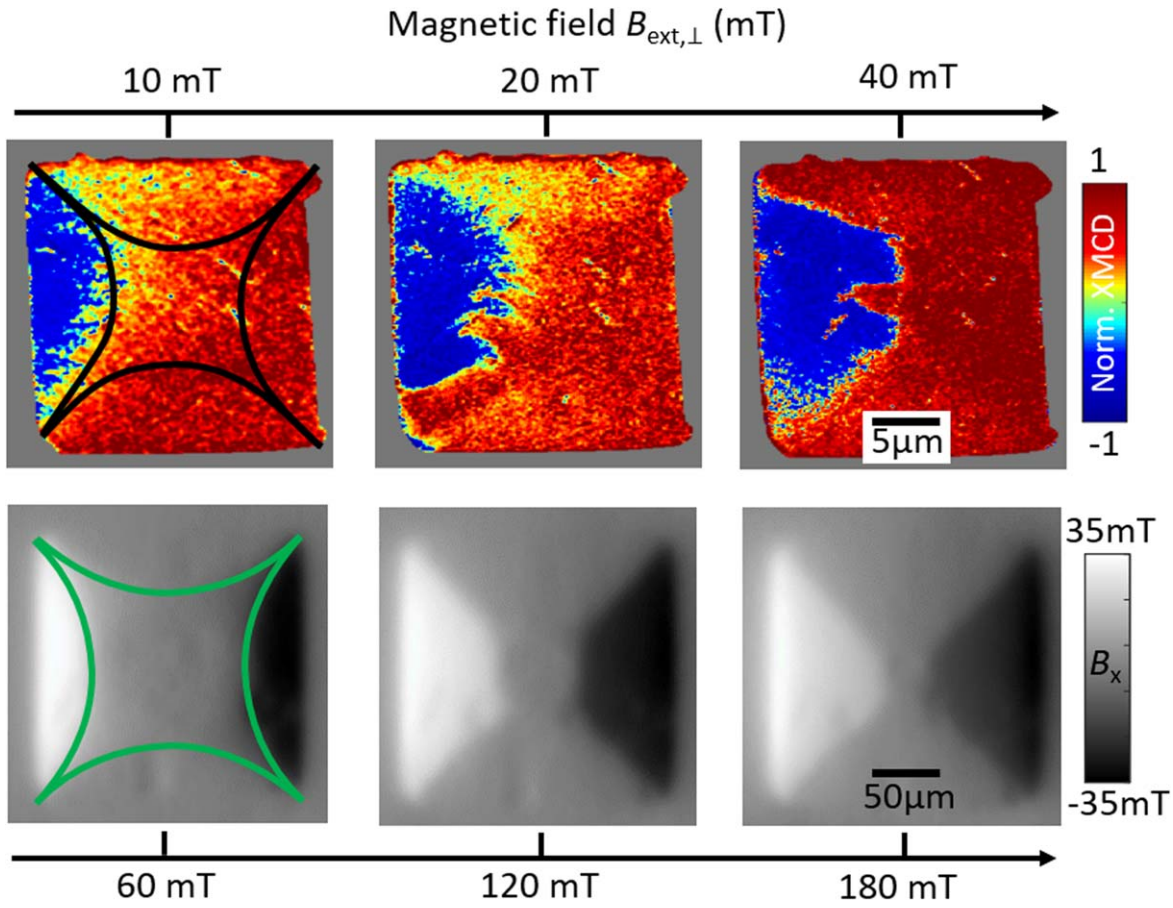

Figure 4. (Top row) Local XMCD pattern in a 20 × 20 μm^2 YBCO(430 nm)/Py(50 nm) bilayer after zero-field cooling to $T = 39$ K. By applying an external field $B_{ext,\perp}$ magnetic flux is forced into the sample. The positions of the flux front and the emerging d-lines are marked by black/green lines. (Bottom row) Magneto-optical micrographs of an equally treated square with ten times larger lateral size (200 × 200 μm^2). Obviously, flux penetrates much easier into the smaller structure.

Since the ferromagnetic layer has been set into the remanent state (red) this measurement is only sensitive to regions of opposite magnetization (blue). Thus, for increasing external fields only the left triangular domain appears. Owing to the overall homogeneous and in-plane-isotropic properties, this experiment is ideal to compare the propagation of the flux front introduced by sweeping the external magnetic field.

The pictures in the bottom row of figure 4 are obtained by magneto-optical Faraday effect microscopy with quantitative analysis [3]. Depicted is the in-plane component B_x of the superconductor stray field in a 200 × 200 μm^2 square. As expected, much higher fields are needed to force magnetic flux into the larger element.

For estimating the position of the flux front in the square we use the theoretical calculations by Brandt *et al* [33], developed for an infinite strip. Here, the position of the flux front P as function of the external magnetic field $B_{ext,\perp}$ is described as:

$$P(B_{ext,\perp}) = (A - A/[\cosh(B_{ext,\perp}/B_c)])/2$$
$$B_c \propto J_c^* d_{YBCO}^* \mu_0^* \ln(2\ A/d_{YBCO}), \quad (1)$$

where d_{YBCO} denotes the thickness of the YBCO film, A the edge length of the square and μ_0 the vacuum permeability. The factor $\ln(2A/d_{YBCO})$ accounts for the finite thickness of the used films, whereby flux is supposed to penetrate easier into smaller elements.

Figure 5 depicts the measured (symbols) and calculated (solid lines) penetration flux fronts for square shape elements with lateral size of 5000 μm (green), 100 μm (blue) and 20 μm (black) in increasing external field $B_{ext,\perp}$. For the calculation we used a critical current density of about 4^*10^{11} A m^{-2} which agrees with corresponding SQUID results.

As predicted by the model of Brandt, we find enhanced penetration of magnetic flux in elements with reduced lateral size. However, the calculated positions of the flux fronts do not coincide with the measured data. The difference (red striped area) is rather small for elements with lateral size of 5000 μm and 100 μm, respectively, while it becomes tremendously enlarged in the 20 × 20 μm^2 square. Thus, the genuine Brandt model does not describe the properties of the supercurrents in this micron-sized SC/FM element.

We attribute this finding to in-plane components of the magnetic field. These components originate from two effects:

First, the magnetic stray field of the superconducting film is not oriented perpendicular to the film plane but shows a complex three-dimensional geometry. The in-plane component at the surface of the superconducting film in the critical

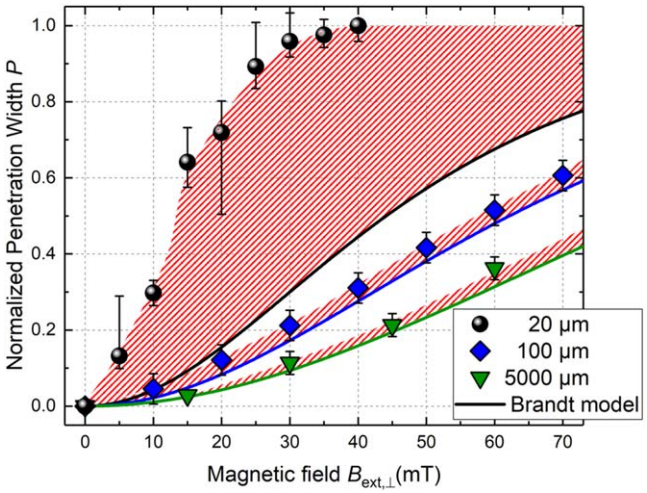

Figure 5. Penetration width P as function of external magnetic field in a YBCO(430 nm)/Py(50 nm) bilayer with lateral size of 5000 μm (green triangles), 100 μm (blue diamonds) and 20 μm (black circles) measured at $T = 26$ K. With reduced lateral size of the elements, flux penetration is enhanced, as predicted by theory (solid lines, see equation (1)). However, we find a difference between measured and calculated data (red striped area), which is dramatically enlarged for the smallest (20 μm) square.

state is constant and proportional to the sheet current [9]. In contrast, the out-of-plane component increases with the lateral size of the film [32]. Thus, largest deviations from the out-of-plane orientation of the local magnetic field occur for small superconducting elements with strong flux line pinning. In this case the orientation of the magnetic field is rotated towards the film plane [33, 34].

Second, the presence of a soft-magnetic cover layer with high magnetic susceptibility further amplifies the in-plane field component. This leads in particular to a modification of the local field geometry and, thus, to a change in flux penetration. Phenomenologically, this can be described by an effective demagnetization factor. This means, flux penetration into small SC/FM bilayers with strong flux line pinning exhibits a more complex behavior due to local occurrence of oblique magnetic fields [35, 36]. Origin of the additional in-plane field of the ferromagnet are deviations of the ideal geometry. The demagnetization factor of a thin infinite film is zero, leading to a vanishing stray field. In our case the roughness of the YBCO-interface as well as the step at the edge of the square (see figure 1) create finite values of the stray field. However, these fields will be significantly smaller than the magnetization of Py ($M \sim 800$ G). We estimate them to be in the order of a few millitesla.

A theory modeling all aspects of flux penetration into SC-elements in oblique magnetic fields was introduced by Mikitik and Brandt [37–39]. Their model proposes enhanced flux penetration in case of an oblique magnetic field which points along the same direction as the flux penetration (towards the center of the element). Therefore, while increasing the external magnetic field, flux has to penetrate faster into the superconductor in comparison to the situation for decreasing the field where an additional repulsion should be present. This theory is not directly applicable to the samples investigated in this work. It describes single-layer superconductors with a thickness larger than the London penetration depth (~800 nm in YBCO along c-axis). Here, bilayers are considered including a superconducting component with a thickness of less than the London penetration depth. Additionally, there is a significant difference between an external applied oblique magnetic field (see Mikitik/Brandt) and the tilting of the local fields introduced by the soft ferromagnet in small SC/FM bilayers. However, the model by Mikitik and Brandt can be seen as a concept for a qualitative explanation of the findings in our system.

To compare flux penetration for opposite directions of field sweep we perform an additional x-ray experiment with a different YBCO/Py bilayer. The lateral size is again 20×20 μm but the YBCO thickness is only 250 nm. The black solid lines in figure 6 mark the position of the flux front which form when the external field is increased (left) or decreased (right) by a finite step of $\Delta B = \pm 20$ mT. The experiment is performed after complete flux penetration, e.g. the superconductor is in the critical state. In the genuine Brandt [40]/Bean [41] model the two flux fronts should exactly coincide.

The panels in figure 6 show that the direction of field sweep significantly affects the flux penetration. Clearly, the flux penetration is much more advanced in the picture on the left. The difference between both images is the direction of the supercurrents, which is clockwise (left) and counter clockwise (right), respectively. This leads to an inversion of the in-plane components of the magnetic field at the surface (green arrows in figure 6). The sign change of the in-plane component directly affects the penetration of magnetic flux.

If the flux penetration is compared to the results displayed in figure 5 it is found that the effect of enhancement/reduction of the penetration length is smaller in figure 6. It is important to emphasize that the YBCO thin film in figure 6 is thinner in comparison to the other investigated samples with a thickness of 430 nm. In addition, the critical current density is only of the order of $3^{*}10^{11}$ A m^{-2}. This has two consequences that reduce the observed effect of asymmetric flux penetration. First, the relevant sheet current $j_c^{*}d$ is about a factor of two smaller, second, the aspect ratio of this sample is slightly larger. Since the ratio of length and thickness is the governing property, which leads to the results of figure 5, the anisotropy has to be smaller in the YBCO film depicted in figure 6.

The model by Mikitik and Brandt assumes a constant external oblique magnetic field, which leads to a point-symmetric flux density distribution inside the superconductor. In our experiment the external field is applied perpendicular to the plane of the sample. Here, the local oblique field is created by the stray field of the supercurrents that locally tilt the total field towards the plane of the film, leading to an axis-symmetric situation. This effect is amplified by the ferromagnetic layer in the vicinity of the SC/FM interface. In addition, the

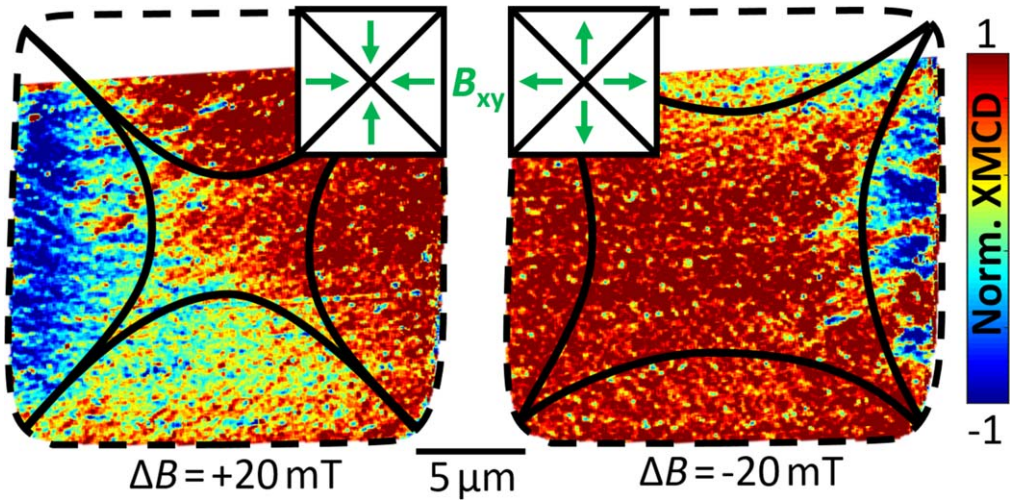

Figure 6. Local XMCD pattern inside the YBCO(250 nm)/Py(50 nm) bilayer at $T = 26$ K after zero field cooling. The positions of the flux fronts/d-lines are marked by black lines. (Left) Increasing the external magnetic field from −40 to −20 mT ($\Delta B = +20$ mT) leads to supercurrents flowing clockwise inside the sample. Here, the local magnetic field points towards the center of the square enhancing the penetration of magnetic flux (black lines). (Right) In case of $\Delta B = -20$ mT (+40 to +20 mT) supercurrents flow anti-clockwise, reversing the latter effect.

interface to the ferromagnet is only on one side of the superconductor, which as well breaks the symmetry of the system. However, our results show that the model of Mikitik and Brandt is appropriate to qualitatively explain the asymmetric flux penetration in small SC/FM bilayers. In both cases flux penetration changes due to an (additional) modification of the (local) direction of magnetic fields A sign-dependent answer of the hybrid material to an external field sweep directly is highly desirable for application as sensor element or for (diode like) rectification of alternating fields.

In summary, we have shown that the position of flux fronts in small SC/FM elements is strongly governed by their lateral size. We studied bilayers consisting of the strong-pinning superconductor YBCO with BYNTO nano-precipitates covered with a ferromagnetic Py layer by means of MSTXM microscopy. In micro-sized structures, a type II superconductor in the critical state cannot be described by the Brandt/Bean model. Additionally, flux penetration exhibits an asymmetric behavior depending on the direction of field sweep. We explain both phenomena by a local oblique magnetic field, which occurs due to deviations from the out-of-plane orientation of the local magnetic field in small superconducting elements and the presence of a soft-magnetic cover layer with high magnetic susceptibility, which further amplifies the in-plane field component. The resulting in-plane components of the magnetic field change the velocity of flux penetration.

Acknowledgments

The authors are grateful to S Ruoß, U Eigenthaler, B Stuhlhofer and T Meisner (MPI Stuttgart) for their contributions to the sample fabrication, J Hänisch (KIT) for the excellent BYNTO:YBCO films, M Bihler and A M Ionescu for fruitful discussions (MPI Stuttgart).

ORCID iDs

J Albrecht https://orcid.org/0000-0002-4047-4302

References

[1] Blatter G, Feigel'man M V, Geshkenbein V B, Larkin A I and Vinokur V M 1994 *Rev. Mod. Phys.* **66** 1125
[2] Brandt E H 1995 *Rep. Prog. Phys.* **58** 1465
[3] Jooss C, Albrecht J, Kuhn H, Leonhardt S and Kronmüller H 2002 *Rep. Prog. Phys.* **65** 651–788
[4] Simmendinger J, Ruoss S, Stahl C, Weigand M, Gräfe J, Schütz G and Albrecht J 2018 *Phys. Rev.* B **97** 134515
[5] Ruoß S, Stahl C, Weigand M, Schütz G and Albrecht J 2015 *Appl. Phys. Lett.* **106** 22601
[6] Stahl C, Walker P, Treiber S, Christiani G, Schütz G and Albrecht J 2014 *Europhys. Lett.* **106** 27002
[7] Stahl C *et al* 2014 *Phys. Rev.* B **90** 104515
[8] Palau A *et al* 2016 *Adv. Sci.* **3** 1600207
[9] Laviano F, Botta D, Chiodoni A, Gerbaldo R, Ghigo G, Gozzelino L and Mezzetti E 2003 *Phys. Rev.* B **68** 014507
[10] Wells F S, Pan A V, Wang X R, Fedoseev S A and Hilgenkamp H 2015 *Sci. Rep.* **5** 8677
[11] Wiemann Y, Simmendinger J, Clauss C, Bogani L, Bothner D, Koelle D, Kleiner R, Dressel M and Scheffler M 2015 *Appl. Phys. Lett.* **106** 193505
[12] Thiemann M, Beutel M H, Dressel M, Lee-Hone N R, Broun D M, Fillis-Tsirakis E, Broschker H, Mannhart J and Scheffler M 2018 *Phys. Rev. Lett.* **120** 237002
[13] Vlasko-Vlasov V K, Colauto F, Benseman T, Rosenmann D and Kwok W-K 2016 *Sci. Rep.* **6** 36847
[14] Opherden L *et al* 2016 *Sci. Rep.* **6** 21188
[15] Sieger M *et al* 2015 *IEEE Trans. Appl. Supercond.* **27** 6601407
[16] Ercolano G, Bianchetti M, Wimbush S C, Harrington S A, Wang H, Lee J H and MacManus-Driscoll J L 2011 *Supercond. Sci. Technol.* **24** 095012
[17] MacMannus-Driscoll J L *et al* 2004 *Nat. Mater.* **3** 439–43
[18] Atkinson D, Allwood D A, Xiong G, Cooke M D, Faulkner C. C and Cowburn R P 2003 *Nat. Mater.* **2** 85–7
[19] Trunk T and Redjdal M 2001 *J. Appl. Phys.* **89** 7606

[20] Soltan S, Albrecht J and Habermeier H U 2004 *Phys. Rev.* B **70** 144517
[21] Dorosinskii L A, Indenbom M V, Nikitenko V I, Ossip'van Y A and Vlasko-Vlasov V K 1992 *Physica* C **203** 149
[22] Keskinbora K, Grévent C, Eigenthaler U, Weigand M and Schütz G 2013 *ASC Nano* **7** 9788–97
[23] Ruoß S, Stahl C, Weigand M, Zahn P, Bayer J, Schütz G and Albrecht J 2016 *New J. Phys.* **18** 103044
[24] Mayer J, Giannuzzi L A, Kamino T and Michael J 2007 *MRS Bull.* **32** 400–7
[25] Brisbois J *et al* 2016 *Sci. Rep.* **6** 27159
[26] Moshchalkov V V, Golubovic D S and Morelle M 2009 *C. R. Phys.* **7** 86–98
[27] Hals K M D, Schecter M and Rudner M S 2016 *Phys. Rev. Lett.* **117** 017001
[28] Stahl C, Gräfe J, Ruoß S, Zahn P, Bayer J, Simmendinger J, Schütz G and Albrecht J 2017 *AIP Adv.* **7** 105019
[29] Buzdin A I 2005 *Rev. Mod. Phys.* **77** 935–76
[30] Schuster T, Indenbom M V, Koblischka M R, Kuhn H and Kronmüller H 1994 *Phys. Rev.* B **49** 3443–52
[31] Albrecht J, Djupmyr M and Brück S 2007 *J. Phys.: Condens. Matter* **19** 216211
[32] Brandt E H and Indenbom M V 1993 *Phys. Rev.* B **48** 12893
[33] Brandt E H, Indenbom M V and Forkl A 1993 *Europhys. Lett.* **22** 735
[34] Brandt E H 1996 *Phys. Rev.* B **54** 4246
[35] Gheorghe D G, Menghini M, Wijngaarden R J, Brandt E H, Mikitik G P and Goldacker W 2006 *Phys. Rev.* B **73** 224512
[36] Vlasko-Vlasov V K, Colauto F, Buzdin A A, Carmo D, Andrade A M H, Oliveira A A M, Ortiz W A, Rosenmann D and Kwok W K 2016 *Phys. Rev.* B **94** 184502
[37] Mikitik G P, Brandt E H and Indenbom M 2004 *Phys. Rev.* B **70** 014520
[38] Brandt E H and Mikitik G P 2005 *Phys. Rev.* B **72** 024516
[39] Mikitik G P, Mawatari Y, Wan A T S and Sirois F S 2013 *IEEE Trans. Appl. Supercond.* **23** 8001920
[40] Brandt E H 1998 *Phys. Rev.* B **58** 6506
[41] Bean C P 1964 *Rev. Mod. Phys.* **36** 31